

# INTERNATIONAL SOCIETY FOR SOIL MECHANICS AND GEOTECHNICAL ENGINEERING



*This paper was downloaded from the Online Library of the International Society for Soil Mechanics and Geotechnical Engineering (ISSMGE). The library is available here:*

<https://www.issmge.org/publications/online-library>

*This is an open-access database that archives thousands of papers published under the Auspices of the ISSMGE and maintained by the Innovation and Development Committee of ISSMGE.*

# Multiscale simulation of flood-induced failure of geosystems

## Multiscale simulation des crues induites par l'échec de geosystems

U. El Shamy

*Southern Methodist University, Dallas, TX, USA*

### ABSTRACT

In this paper, flood-induced failure of a hydraulic structure was simulated using a three-dimensional transient fully-coupled hydromechanical model taking into account the fluid-soil-structure interactions. The fluid was idealized as a continuum by using averaged Navier-Stokes equations that accounts for the presence of the solid particles. The discrete element method (DEM) was employed to model the assemblage of these particles. The interphase momentum transfer was modeled using an established relationship that considers the dynamic change in porosity and possible occurrence of nonlinear losses. Computational simulation was conducted to investigate the response of a hydraulic structure founded on a granular deposit when subjected to a rapidly increasing hydraulic head difference. The conducted simulation provided information at the micro-scale level for the solid phase as well as at the macroscopic level for the pore-water flow. The settlement and failure mechanism of the structure was captured. The proposed computational framework for analyzing river and flood-protection levees provides a new dimension to the analysis and design of such vital geotechnical systems.

### RÉSUMÉ

Dans ce document, les inondations induites par l'échec d'une structure hydraulique a été simulée en utilisant un passage en trois dimensions entièrement hydromécanique associée modèle en tenant compte de la sol-fluide-structure interactions. Le liquide était idéalisé comme un continuum, en utilisant la moyenne des équations de Navier-Stokes que les comptes de la présence de particules solides. Le discrete element method (DEM) a été utilisé pour modéliser l'assemblage de ces particules. L'interface dynamique de transfert a été modélisé en utilisant des relations bien établies qui considère la dynamique de changement de la porosité et de la possible survenue nonlinear pertes. Computational simulation a été réalisée pour étudier la réponse d'une structure hydraulique fondé sur un dépôt granulaire sous l'effet d'une augmentation rapide hydraulique différence. La simulation effectuée a fourni des informations au niveau micro-échelle pour la phase solide ainsi que par l'échelle macroscopique des pores pour le débit d'eau. Le mécanisme de règlement et l'échec de la structure a été capturé. Le projet de cadre pour l'analyse de calcul rivière et les inondations des digues de protection offre une nouvelle dimension à l'analyse et la conception de ces systèmes vitaux géotechniques.

Keywords : Navier-Stokes equations, seepage, granular media, transient flow, discrete elements

## 1 INTRODUCTION

Flood-induced piping and subsequent formation of sand boils is a major cause of severe damage to river levees and earth dams. Most of the analytical work found in the literature considers piping under steady-state conditions (Sellmeijer and Koenders, 1991; Ojha et al., 2003). While these models can be used for the design of levees against piping, they do not account for intergranular stresses, stresses due to the weight of the hydraulic structure, and/or any subsequent deformation of the soil system. Application of computational methods in modeling of piping is widely used. Griffiths and Fenton (1997, 1998) employed two- and three-dimensional finite element models to study seepage in spatially random soil with statistically variable soil permeability and steady-state flow. Unsteady ground water flow models using the finite element method were also presented (e.g., Nath, 1981; Koo and Leap, 1998). Lu and Zhang (2002) used the finite difference technique that accounts for heterogeneous soils.

Flow conditions that would result in piping encompass several issues that have to be accounted for when developing a computational model for fluid flow through a deforming porous medium. In the case of flood-induced piping, transient analysis has to be considered since flooding of a river results in a rapidly increasing hydraulic head that a steady flow regime is unlikely to occur. Furthermore, under such extreme flow conditions, soil particles may undergo large displacements leading to significant changes in porosity. Variations in porosity affect the soil

hydraulic conductivity and deformation characteristics. The effects of the weight of the hydraulic structure on the developed stresses within the soil mass during water flow have to be taken into account.

Conceptually, in presented computational framework, the mixture of solid particles and pore fluid can be viewed as two interpenetrating media, namely the solid phase and the fluid phase. The fluid is idealized as a continuum by using a homogenized form of Navier-Stokes equations that accounts for the presence of the solid particles. These particles are modeled at a micro-scale using the discrete element method (DEM). The inter-phase momentum transfer is modeled using an established relationship. The soil-structure interaction is maintained by generating a clump which behaves as a rigid body. The model is discussed briefly in the following section followed by results of the computational simulation.

## 2 METHODOLOGY

Saturated granular soils were idealized as two overlapping media. The solid phase was modeled as an assemblage of discontinuous particles using the discrete element method, DEM (Cundall and Strack 1979). The pore fluid was considered to be inviscid and incompressible, and was idealized using averaged Navier-Stokes equations of conservation of mass and momentum (e.g., Jackson, 2000):

$$\frac{\partial n}{\partial t} + \frac{\partial(nu_i)}{\partial x_i} = 0 \quad (1)$$

$$\frac{\partial(nu_i)}{\partial t} + \frac{\partial(nu_i u_j)}{\partial x_j} = -\frac{n}{\rho} \frac{\partial p}{\partial x_i} + n\rho g_i + d_i \quad (2)$$

In Eqs. (1) and (2):  $x_i$  ( $i=1,2,3$ ) are Cartesian coordinate,  $t$  is time,  $n$  is porosity,  $u_i$  is fluid velocity,  $\rho$  is fluid density,  $p$  is fluid pressure, and  $g_i$  is gravitational force per unit mass. The term  $d_i$  represents averaged fluid-particle interaction force per unit of volume and was accounted for by using well established semi-empirical relationships proposed by Ergun (1952).

An explicit time-integration scheme is used to evaluate the coupled fluid-particle response (Itasca, 2005). The fluid domain is discretized into parallelepiped cells and averaged Navier-Stokes equations are solved using a finite volume technique. Average drag forces exerted by the fluid on the particles within a specific cell were evaluated based on mean values of porosity, as well as of particle sizes and velocities within this cell. These forces were then applied to each of the individual particles proportionally to their volumes. Deformation of the solid phase subjected to the drag forces along with any external loads was subsequently computed using DEM (Itasca, 2005). Further details of the implemented continuum-discrete model are given in (El Shamy and Aydin, 2008).

### 3 SIMULATION

The proposed approach was used to conduct a computational simulation of seepage through a deforming granular medium. A hydraulic structure with a length of 5.0 m was constructed over a 9.7 m deep deposit of cohesionless soil. The total number of particles that can be used reasonably in a DEM simulation using current state-of-the-art serial computers is small in comparison to the number of grains comprised in an actual deposit. Therefore, the high-g level concept commonly implemented in centrifuge modeling was utilized. Uniformly graded spherical soil particles with a uniformity coefficient of 1.4 were generated and settled under 1 g until there was no further movement of particles. Then a 100 g gravitational field was applied until a submerged state condition was maintained (Fig. 1). In order to compensate for the employed high g-level, viscous fluid was used in the simulation (Kutter, 1992).

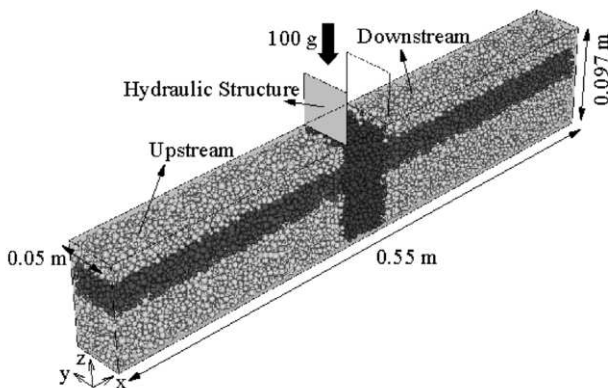


Figure 1. Three-dimensional view of the simulated particulate deposit (dimensions are in model units).

#### 3.1 Modeling the hydraulic structure

The hydraulic structure was generated using clumped spherical particles such that it behaves as a rigid body (a clump). That is, regardless of the forces acting upon it, the structure will not

break apart. The contact forces between the clumped particles are not taken into account. However, the interactions between the clumped particles and soil particles are considered. The spherical clumped particles were assembled to resemble near-realistic conditions between the hydraulic structure and the soil particles. The stress applied by the structure on the underlying soil resembled that due a structure that is 6.5 m high, 5 m wide, and with a 2000 kg/m<sup>3</sup> material density. Only a 5 m strip was considered in the normal direction to analyze the presumably infinite structure.

Forces that act on the structure were calculated analytically and were taken into account during the course of the simulation (Fig. 2). In this figure, L, H, and B represent, respectively, the length, height and width of the structure and  $H_w$  is the height of the water level.  $W$  is the self weight of the structure,  $p$  is the water pressure for corresponding  $H_w$ ,  $U$  is the uplift force,  $F_x$  is the horizontal force due to water pressure,  $F_r$  is the frictional force between the hydraulic structure and the soil particles and  $M$  is the moment created on the centroid of the structure as a result of these forces. In the simulation, forces acting on the structure as well as their turning moments were calculated as the water level increased and carried to the centroid of the structure. The frictional force  $F_r$  was obtained from the contact forces of particles in contact with the base of the structure and was automatically accounted for. Since the clump behaves as a rigid body, translational and rotational motion equations are sufficient to describe its motion (Itasca, 2005).

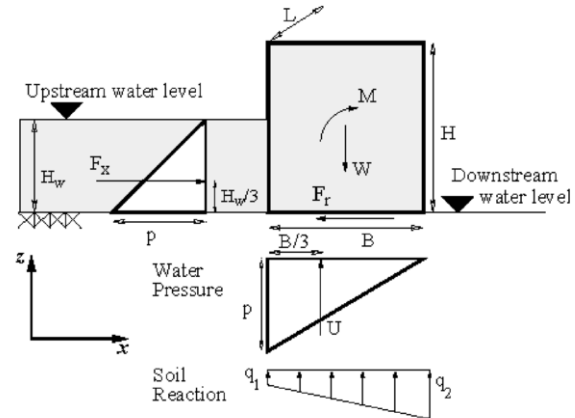


Figure 2. Free body diagram of the forces acting on the hydraulic structure.

After generating the particles composing the structure, the deposit was allowed to come to equilibrium. The initial conditions were chosen to correspond to an initial head difference of approximately 1.0 m and the fluid flow was allowed to reach steady state under these conditions. The deposit was then subjected to a head increase at a rate of 100 Pa per second. Multiple solid and pore-fluid state variables were monitored during the course of the simulation. Table 1 summarizes the computational data for the solid and fluid phases as well as other computational details. Results are presented in prototype units exclusively.

#### 3.2 Soil-structure response to water rise in the upstream

The structure was subjected to an incremental increase in the upstream water level while maintaining the downstream water level at a constant height of 1.0 m. The progressive increase in the uplift pressure underneath the hydraulic structure is shown in Fig. 3 at selected time instants of head increase. Due to the soil-fluid-structure interactions, any deformation of the solid phase caused the structure to experience displacement and rotation (Fig. 4). Soil particles in this simulation were not only under the effect of their own weight and fluid flow, but also the stresses induced by the weight of the hydraulic structure. The

first significant settlement, which may be considered as the failure of the structure, was observed at a water height of about 2.6 m (Fig. 5). Complete failure occurred just after 3 seconds at about 4.1 m upstream water level. These findings show the fact that failure can happen at hydraulic gradients that are significantly lower than the critical value as discussed below.

Table 1. Characteristics of conducted numerical simulation.

Particles	
Diameter	1.7 mm to 8.5 mm
Normal/Shear Stiffness	$10^5$ N/m
Friction coefficient	0.5
Density	$2650 \text{ kg/m}^3$
Number of particles	22,303
Fluid (water at 20°C)	
Density	$1000 \text{ kg/m}^3$
Viscosity	0.1 Pa s
Structure	
Width (y-dir.)	50 mm
Depth (z-dir.)	65 mm
Length (x-dir.)	50 mm
Density of a clump particle	$12.92 \text{ Mg/m}^3$
Computation parameters	
Time steps for DEM	$4 \times 10^{-4}$ s
Time steps for fluid	$2 \times 10^{-5}$ s
Number of fluid cells	$44 \times 3 \times 8$

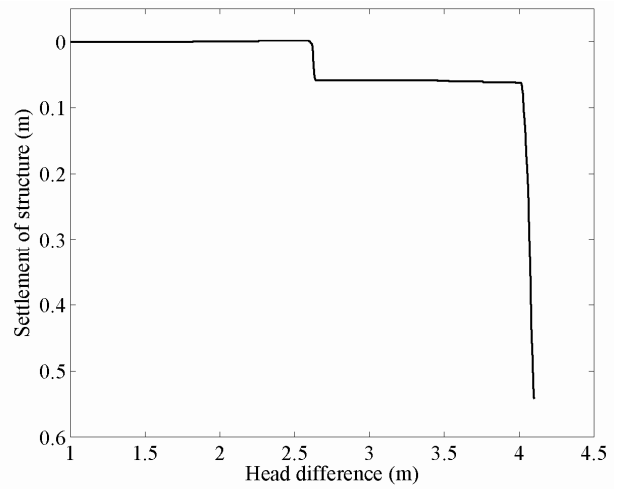


Figure 5: Settlement of the hydraulic structure in the vertical direction with the increase in head.

The most commonly used criterion in geotechnical engineering to assess the susceptibility of a soil deposit to piping is based on evaluating the safety factor against piping defined as the critical gradient divided by the hydraulic gradient. The critical gradient estimated from Terzaghi's classical formula (Terzaghi and Peck, 1967) is given by:

$$i_c = \frac{(\gamma_s - \gamma_w)}{\gamma_w} (1 - n) \tag{3}$$

where,  $i_c$  is the critical gradient,  $\gamma_s$  is the specific weight of soil particles, and  $\gamma_w$  is specific weight of water. Thus, the critical gradient as defined by Eq. 3 is a macro-scale material property that depends mainly on porosity. In the present simulation, the critical location for piping to take place is at the toe of the structure on the downstream side. To assess the factor of safety against piping in that location, the changes in porosity and the corresponding critical gradient as well as the hydraulic gradient were produced as the head difference increased (Figs. 6 and 7).

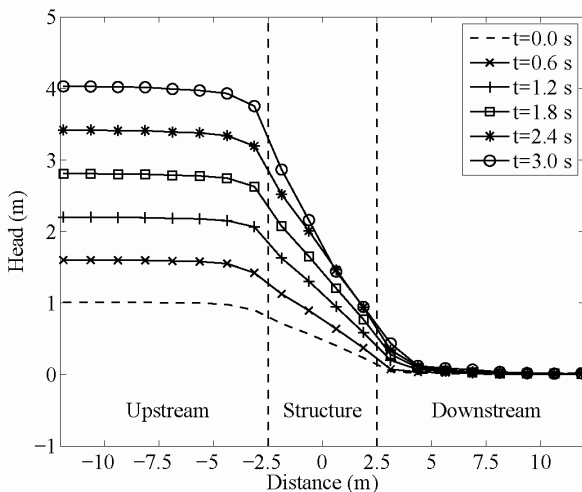


Figure 3. Progressive increase in head difference with time in the vicinity of the hydraulic structure.

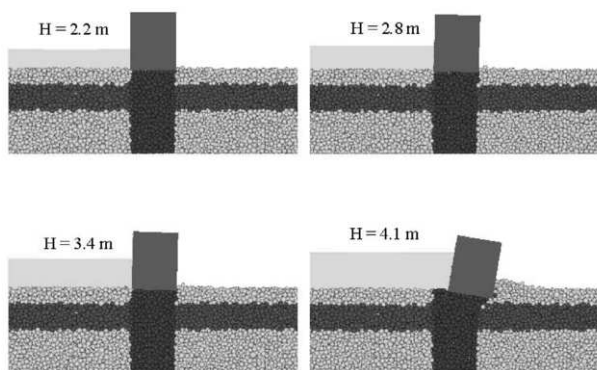


Figure 4. Snapshots of particles and hydraulic structure at selected instants of head difference increase (H).

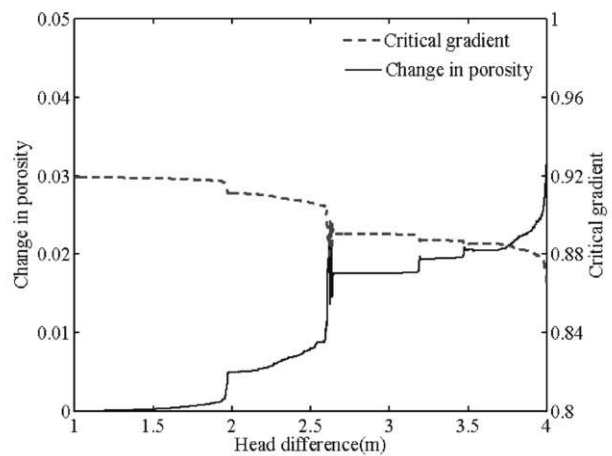


Figure 6. Changes in porosity and critical gradient at the toe of the structure on the downstream side with the increase in head difference.

The initial value of the critical gradient at the toe of the structure was about 0.92. As indicated by Fig. 6, the soil at the toe of the structure on the downstream side experienced a volume increase particularly around the time of first significant settlement of the structure ( $H=2.6$  m). During the course of the simulation, the smallest value of the safety factor was about 1.9 (at  $H=4.0$  m). At the time of significant settlement of the structure ( $H=2.6$  m) the factor of safety was about 2.5, implying

that the soil near the toe of the structure is safe against piping (Fig. 7). It may be then concluded that the settlement of structure, and its subsequent failure, can not be solely attributed to the formation of piping.

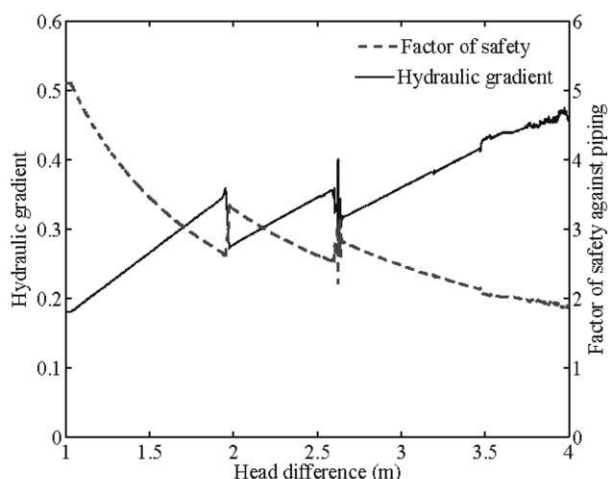


Figure 7. Variation of hydraulic gradient and safety factor against piping at the toe of the structure on the downstream side with the increase in head difference.

Soil deformation is a result of the stresses induced by the hydraulic structure as well as by the flowing water. The stresses due to the structure are not constant with time as the structure is subjected to increasing hydrostatic and uplift pressures. While the increase in uplift pressure would tend to reduce the structure-induced stresses within the soil, the turning moments due to the hydrostatic and uplift pressures tend to overturn the structure around its toe causing stresses to increase at that location and the particles directly under the toe of the structure to move downward. On the other hand, water flow applies mostly upward forces at the exit face near the toe of the structure on the downstream side producing a tendency to lift the particles at the exit face. This combined effect of downward pressure from the structure and upward drag forces from water flow at the toe causes the soil particles next to the toe on the downstream side to move upward in a failure mode similar to that of a bearing capacity failure mechanism (Fig. 8). In this figure, it can be seen that there were two instances of failure on two different failure surfaces (indicated by the dashed line on the figure). The first instance occurred as the upstream water level approached a height of 2.6 m. The structure tilted and settled but remained in this new position until the water level reached a height of 4.0 m. Upon reaching this height, another failure plane can be observed where the structure experienced excessive tilting and displacement.

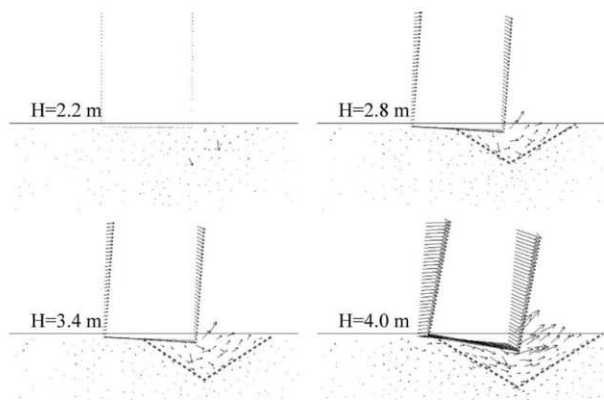


Figure 8. Snapshots of accumulated soil particles and structure displacement vectors at selected head increase instants (maximum amplitude=1.0 m).

#### 4 CONCLUSION

This paper examines the potential of a three-dimensional fully-coupled fluid-particle-structure model to simulate large soil deformations resulting from extreme flow conditions. The approach accounts for soil-structure interaction, transient flow conditions, spatial and time variations in porosity and subsequent changes in the permeability of the soil. The mesh-free nature of DEM allows particle movements to be tracked as they respond to the seepage forces. The conducted simulation captured the movement of soil particles and the subsequent displacement of the hydraulic structure showing the trend of failure. The failure mechanism of the hydraulic structure due the rapid rise of upstream water level is similar to a bearing capacity failure. The combined action of stresses induced by the structure and water flow may lead to a sudden failure at hydraulic gradients less than the critical gradient. This approach appears to be a very effective tool to model saturated granular deposits when subjected to high seepage forces such as those encountered during flooding of a river.

#### ACKNOWLEDGEMENT

This research was supported by the Louisiana Board of Regents Support Fund, grant number LEQSF(2005-07)-RD-A-32. This support is gratefully acknowledged.

#### REFERENCES

- Cundall, P. A. and Strack, O. D. L. 1979. A discrete numerical model for granular assemblies. *Geotechnique*, 29(1), pp. 47–65.
- El Shamy, U. and Aydin, F. 2008. Multiscale modeling of flood-induced piping in river levees. *Journal of Geotechnical and Geoenvironmental Engineering*, ASCE, 134(9), pp. 1385–1398.
- Ergun, S. 1952. Fluid flow through packed columns. *Chemical Engineering Progress*, 43(2), pp. 89–94.
- Griffiths, D. V. and Fenton, G. A. 1997. Three-dimensional seepage through spatially random soil. *Journal of Geotechnical and Geoenvironmental Engineering*, ASCE, 123(2), pp. 153–160.
- Griffiths, D. V. and Fenton, G. A. 1998. Probabilistic analysis of exit gradients due to steady seepage. *Journal of Geotechnical and Geoenvironmental Engineering*, ASCE, 124(9), pp. 789–797.
- Itasca 2005. Particle Flow Code, PFC3D, release 3.1. Itasca Consulting Group, Inc., Minneapolis, Minnesota.
- Jackson, R. 2000. *The dynamics of fluidized particles*. Cambridge, U.K.; New York: Cambridge University Press, London, UK.
- Koo, M. H. and Leap, D. I. 1998. Modeling three-dimensional groundwater flows by the body-fitted coordinate (BFC) method: II. free and moving boundary problems. *Transport in Porous Media*, 30(3), pp. 345–362.
- Kutter, B. 1992. Dynamic centrifuge modeling of geotechnical structures. *Transportation research record*, (1336), pp. 24–30.
- Lu, Z. and Zhang, D. 2002. Stochastic analysis of transient flow in heterogeneous, variably saturated porous media: the van Genuchten-Mualem constitutive model. *Vadose Zone Journal*, 1, pp. 137–149.
- Nath, B. 1981. A novel finite element method for seepage analysis. *International Journal for Numerical and Analytical Methods in Geomechanics*, 5, pp. 139–163.
- Ojha, C. S. P., Singh, V. P., and Adrian, D. D. 2003. Determination of critical head in soil piping. *Journal of Hydraulic Engineering*, ASCE, 129(7), pp. 511–518.
- Sellmeijer, J. B. and Koenders, M. A. 1991. A mathematical model for piping. *Applied Mathematical Modeling*, 15(6), pp. 646–651.
- Terzaghi, K. and Peck, R. 1967. *Soil mechanics in engineering practice*. John Wiley and Sons, New York, NY.